CONF-9004254--1
PNL-SA-17971

PNL-SA--17971

DE91 005247

KEY STRUCTURE-ACTIVITY RELATIONSHIPSS IN THE VANADIUM PHOSPHORUS OXIDE CATALYST SYSTEM

M. R. Thompson
J. R. Ebner

April 1990

Presented at the
American Chemical Society, Spring Meeting,
Boston 1990
April 22-27, 1990
Boston, Massachusetts

Work supported by the
U. S. Department of Energy
under Contract DE-AC06-76RLO 1830

Pacific Northwest Laboratory
Richland, Washington 99352

Final Draft:
R.S. Grasselli, A.W. Sleight (Editors), Studies in Surface Science and Catalysis,
"*Structure-Activity Relationships in Heterogeneous Catalysts*", Elsevier, Amsterdam

KEY STRUCTURE-ACTIVITY RELATIONSHIPS IN THE VANADIUM PHOSPHORUS OXIDE CATALYST SYSTEM

Jerry R. Ebner, Monsanto Company, 800 North Lindbergh Avenue,
St. Louis, Missouri, 63303

Michael R. Thompson, The Pacific Northwest Laboratory[1],
Battelle Blvd., Richland, Washington, 99352

Abstract

The crystal structure of vanadyl pyrophosphate has been redetermined using single crystals obtained from a near solidified melt of a microcrystalline catalyst sample. Crystals that index as vanadyl pyrophosphate obtained from this melt are variable in color. Crystallographic refinement of the single crystal X-ray diffraction data indicates that structural differences among these materials can be described in terms of crystal defects associated with linear disorder of the vanadium atoms. The importance of the disorder is outlined in the context of its effect on the proposed surface topology parallel to (1,0,0). Models of the surface topology simply and intuitively account for the non-stoichometric surface atomic P/V ratio exhibited by selective catalysts of this phase. These models also point to the possible role of the excess phosphorus in providing site isolation of reactive centers at the surface.

Introduction

The conversion of butane to maleic anhydride on vanadium phosphorus oxide catalysts represents the only commercial process for selective functionalization of an alkane. The catalytic performance of vanadium phosphorus oxide catalysts for this reaction is unequaled by any other metal or metal-oxide system. A large number of published reports attribute catalytic activity/selectivity to the bulk crystalline phase vanadyl pyrophosphate, $(VO)_2P_2O_7$ (2-7). The catalytic performance of vanadyl pyrophosphate is strongly related to the method of preparation employed. For example, vanadyl pyrophosphate catalysts synthesized in aqueous versus organic media have significant catalytic performance differences (6,8-13). In this paper the structural complexities of vanadyl pyrophosphate are explored through single crystal X-ray structural analysis. The single crystal results seem to provide an additional perspective on the differences evidenced in the properties derived from different solvent systems. Further, the results of these crystallographic studies have led us to assemble zeroth-order models of the surface topology parallel to (1,0,0) and to gain some insight into the potential role of the non-stoichometric surface phosphorus in determining selectivity.

Structure-Activity Relationships in VPO Catalysts

The catalysts used in this study were prepared with approximately 10% excess phosphorus in aqueous and organic media according to well-established literature procedures (6). The $[VOHPO_4]_2{\cdot}H_2O$ precursors from the aqueous and organic preparations were dehydrated and partially oxidized by air calcination at

400°C for 1-2 hours. The microcrystalline catalysts described here were formed and characterized after running the butane oxidation reaction at 1.4 - 2.0% butane and 1000 GHSV for approximately 750 continuous hours. Catalyst performance of the organic derived catalyst is 7 absolute yield points superior to the aqueous counterpart over the range of space velocities (Figure 1). Many similarities exist between the two catalyst systems. Both microcrystalline catalysts have a vanadium oxidation state of 4.01 ± 0.01, a bulk

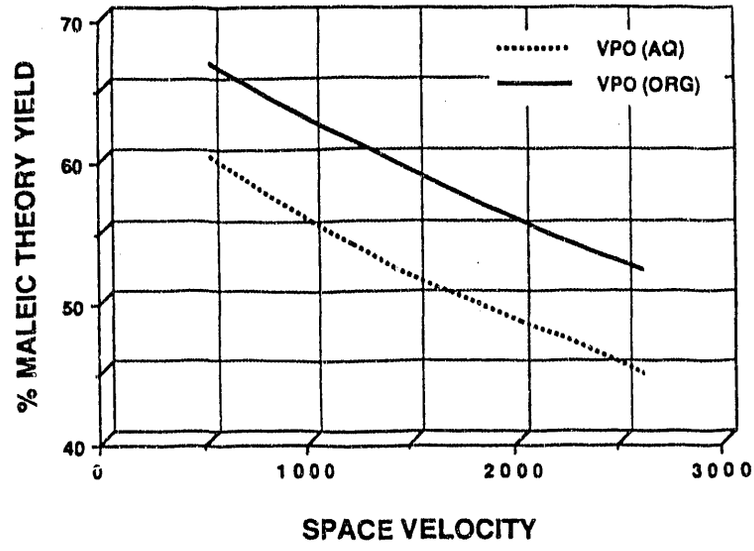

Figure 1. Catalyst performance for aqueous (dotted line) and organic (solid line) derived vanadyl pyrophosphate catalysts.

phosphorus to vanadium ratio of 1.00 ± 0.025, and XPS surface atomic phosphorus/vanadium ratios of 1.5 ± 0.3. There are several measurements that distinguish the two catalyst systems. The BET surface areas are 10 and 14 m^2/g. for aqueous and organic derived catalyst systems, respectively. The SEM determined morphologies of the $[VOHPO_4]_2 \cdot H_2O$ precursors are large hexagonal plates and thin, rose-like platelets for the aqueous and organic catalysts, respectively. However, these major morphological differences are somewhat diminished in the aged catalysts. SEM images indicate in both systems significant fracturing of the platelets and formation of rectangular and rodlike crystal habits 0.1 - 1.0 microns in size, with the organic system having more rods than the aqueous counterpart and generally smaller in size by a factor of two. The previously published XRD patterns (Figure 2a-b) of the resulting aqueous and organic derived catalysts (6) differ in two respects: (1) the overall intensities of the primary peaks in the powder patterns are greater in intensity for the aqueous derived catalyst; and (2) a single reflection at 3.87Å ($2\theta_{CuK\alpha} = 22.90^o$) is significantly broadened in the organic derived catalyst. The latter difference has been attributed to layer stacking disorder in vanadyl pyrophosphate (10,12,14). The exact form of the orientational disorder contributing to this key, distinguishing feature has not previously been reported.

The solid-state structure of vanadyl pyrophosphate has previously been reported (15), but inconsistencies in these studies have generated doubt concerning the accuracy of the crystallographic model. Because, as the previous discussion indicates, the structural nuances of vanadyl pyrophosphate are of such

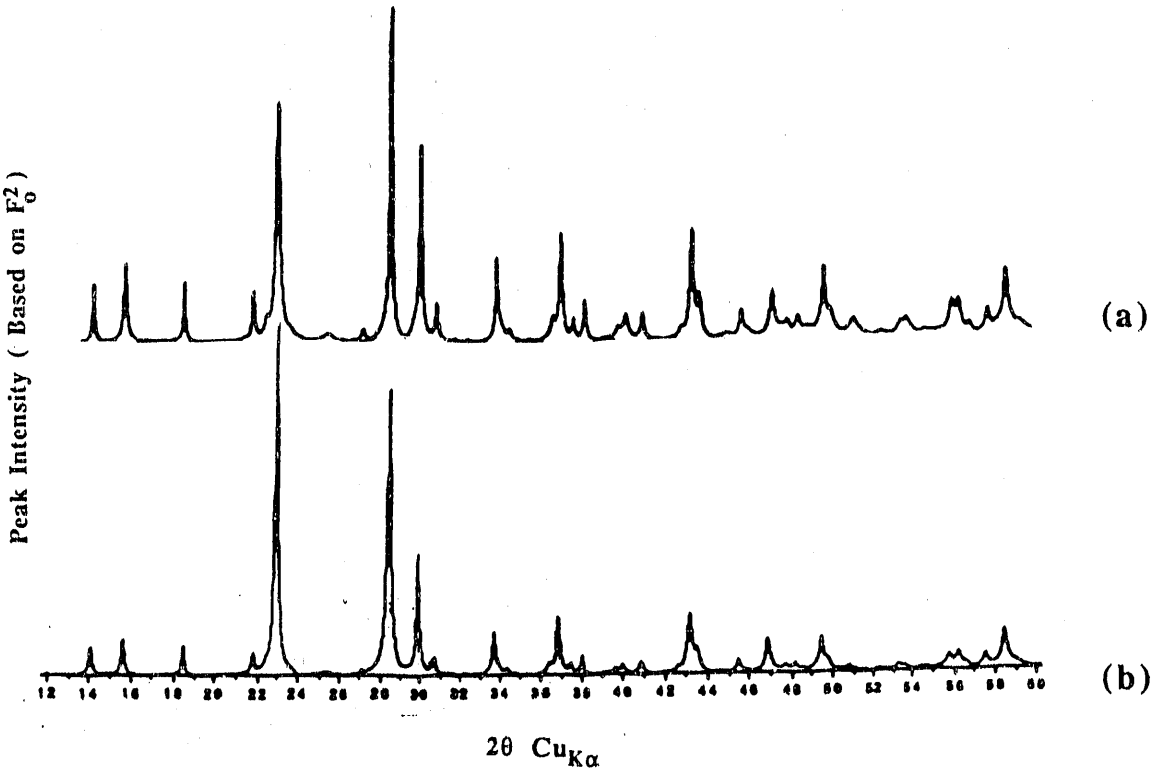

Figure 2. Observed X-ray powder patterns for microcrystalline catalysts prepared in (a) aqueous and (b) organic media.

great importance to catalysis, a re-examination of this structural determination seemed prudent. Thus, single crystals were obtained via a new route: crystal growth from a near-solidified melt of the microcrystalline catalyst. The structural linkage between the synthesized crystals and the microcrystalline catalyst samples was firmly established by comparing crystal and catalyst vibrational spectra using laser Raman and FTIR microprobe techniques. With the new crystals, we have sought to re-determine the crystal structure in order to clarify the origin of apparent crystal defects. In addition, we have made an attempt to assemble zeroth-order models of the surface topology parallel to (1,0,0) which would accommodate the non-stoichometric surface phosphorus. Differences between bulk and surface P/V stoichometry for microcrystalline vanadyl pyrophosphate catalysts have been reported previously (16), as well as the decrease of reaction selectivity associated with surface phosphorus loss during the butane reaction (17). It is clear that any structural model for the catalyst must account for the disposition of excess surface phosphorus, and its role in selectively enhancement.

The Crystal Structure of Vanadyl Pyrophosphate, Revisited

Simultaneously in 1978, Linde and Gorbunova (15a), and separately, Middlemiss (15b), reported the X-ray structure determination of vanadyl pyrophosphate. Unfortunately, the results of both studies possessed serious flaws in their crystallographic models. Middlemiss attempted to phase the structure via Patterson synthesis ("heavy-atom" techniques), which resulted in the refinement of a projection of the structure in the non-centrosymmetric space group $Pbc2_1$ (18a). Linde utilized statistical phasing methods to solve the structure, which resulted in a model with identical connectivity as that described by Middlemiss, and lower residuals: R_1=0.089, and R_w=0.091. However, the Linde model contained several unusual bonding interactions and puzzling pseudo-symmetry. The bonding interactions in question involved the

vanadyl moiety (V=O), which in the fully refined model gave two chemically inequivalent bonds: two in the range of 1.54(2)Å, and the remaining two interactions of approximately 1.72(2)Å. Furthermore, the structure was reported in a brief format with little experimental information.

Diffraction quality crystals of vanadyl pyrophosphate, used to re-determine the crystal structure, have been obtained from near-solidified melts derived from microcrystalline catalyst samples. Recrystallization experiments utilized samples taken from a fixed-bed reactor after more than 5000 hours in the butane oxidation reaction. Surprisingly, the single crystals harvested from these melts, which index as vanadyl pyrophosphate in diffraction experiments, are variable in color, ranging from emerald-green to gray, and from yellow-brown to red-brown. Single crystals described by Linde et al. and Middlemiss were reportedly emerald-green in color. Color variations have been noted previously in the preparation of microcrystalline catalyst materials (19).

Emerald-green crystals of vanadyl pyrophosphate are orthorhombic (20), with a = 7.710(2)Å, b = 9.569(2)Å, c= 16.548(3)Å, V= 1220.9(8)Å^3, ρ_{calc}= 3.359(2) g/cm^3. Red-brown crystals exhibit lattice parameters which are slightly dilated relative to their emerald-green counterparts: a=7.746(2)Å, b= 9.606(2)Å, c=16.598(3)Å, V= 1235.0(8)Å^3, ρ_{calc}= 3.320(2) g/cm^3. Lattice parameters cited by the previous authors are nearly identical to the emerald-green specimens studied here. Aside from the color variation, the intensities and peak widths for numerous reflections collected from the single crystals show marked differences between the materials. These differences are similar to those reported for the X-ray powder diffraction patterns for catalysts prepared from aqueous or organic media. Significant differences also exist in the Raman spectra for emerald-green and red-brown crystals. For example, emerald-green and gray crystals exhibit a strong sharp doublet centered at 922 cm^{-1}, which is diminished to a broad weak singlet at 928 cm^{-1} for the yellow-brown and red-brown materials (21). We believe that the structural differences apparent in these single crystals are likely those which have been identified with the microcrystalline catalysts and relate to the ordering of the metal atoms within the structure.

The diffraction data taken from ten single crystals of vanadyl pyrophosphate have been extensively studied. Due to the complexity of this crystal structure, only a terse discussion of our results will be presented here. Our primary interest was to verify that the solution of the crystal structure reported by Linde was correct, and secondly, to determine the cause of the poor refinement results.

The atomic coordinates reported by Linde indicated strong pseudo-symmetry, especially apparent for the heavy atoms (22), suggestive of higher space group symmetry than that chosen. However, no higher symmetry description of the lattice could be found. The space group extinctions are rigorously consistent only with the choice of P_{ca2_1} or the centrosymmetric counterpart, P_{cam} (18b). Structural solutions for emerald-green and red-brown crystals (and for the data published by Middlemiss) can be found in non-centrosymmetric P_{ca2_1} consistent with structure reported by Linde. While not fully indicative of a correct solution, these twenty-six atom models refine to conventional residuals in the range of R_1=0.089-0.096 and R_w=0.093-0.099 for the crystals studied. A perspective plot of one layer of the structure projected on the bc-plane is illustrated in Figure 3. We have also been able to find numerous solutions to the structure, consistent with the connectivity of vanadyl pyrophosphate, in the centrosymmetric space groups P_{cam} and

P_{caa} (18c). Efforts to refine these centrosymmetric structures have failed to yield models which converge at residuals less than R_1=0.15.

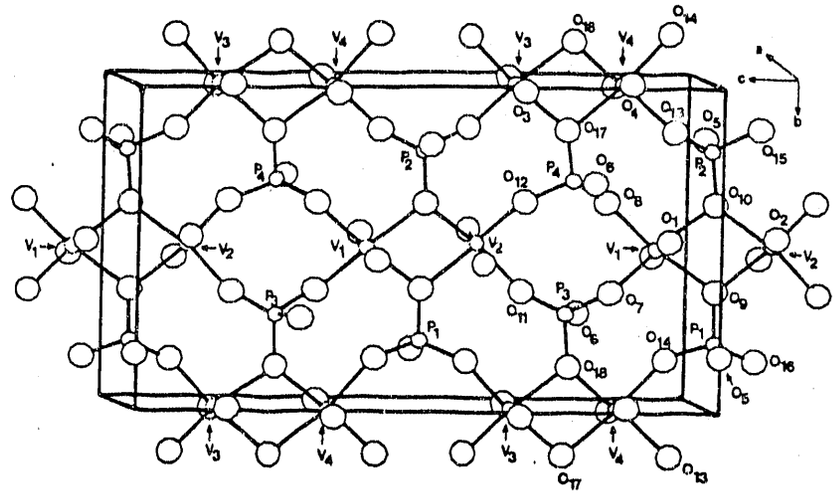

Figure 3. Projection of the continuous structure of vanadyl pyrophosphate onto the crystallographic bc-plane.

Difference Fouriers computed from the twenty-six atom models in P_{ca2_1} for both emerald-green and red-brown crystals indicate residual electron density consistent with disorder of the vanadium sites. The disordered positions for the metal atoms are oriented approximately 0.65Å across the basal plane of the distorted octahedral vanadium coordination sphere. This type of disorder is common for crystal structures which possess square-pyramidally distorted octahedral metal centers and is the cause of the previously reported diffraction streak effects noted in electron diffraction studies of the microcrystalline catalysts (23). For this structure the disorder represents a columnar re-orientation of the vanadyl bonds, reversing the direction of the entire column along the a-axis. It should be noted that for all crystals studied, there is no such disorder indicated for the phosphorus atoms.

In order to better understand the symmetry and structure of the crystallographic model, consider the schematic representation of a small fragment of the continuous solid reported by Linde, depicted in Figure 4.

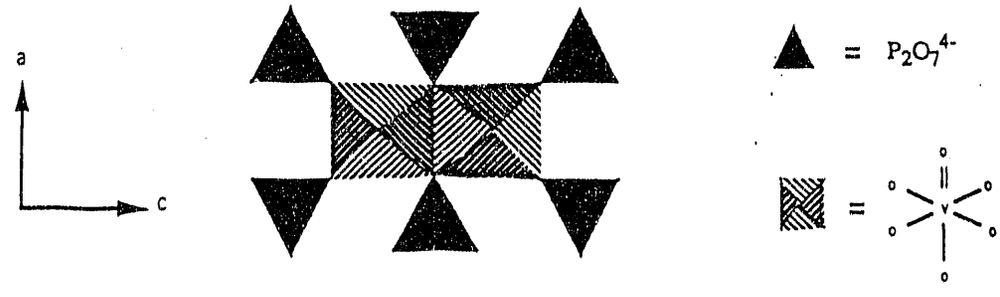

Figure 4. Schematic representation of the vanadium centered dimeric unit which comprises the layered structure of vanadyl pyrophosphate.

Neglecting the exact direction of the vanadyl and pyrophosphate groups, this two-dimensional fragment is representative of the unit of structure comprising the close-packed layers of vanadyl pyrophosphate. The d^1 vanadium centers possess pyramidally distorted octahedral coordination. The structural anisotropy about the metal atom is attributable to the formal double bond between the vanadium and the vanadyl oxygen, and a concomitantly weak interlayer oxygen interaction trans to V=O (24). The close-packed layer structure is comprised of this dimeric unit in which adjacent vanadium centered octahedra share a common polyhedral edge. Each dimer is surrounded by six apex-shared pyrophosphate groups. The pyrophosphate groups form interlayer bonds via the pyrophosphate oxygen (P-O-P), are oriented perpendicular to the plane of the paper in Figure 3, and bridge to adjacent layers above or below the plane. If, for instance, the direction of these six pyrophosphates alternate their orientation relative to the close-packed plane, ie. oriented up-down-up-down-up-down traversing the perimeter of the dimer, then a center of symmetry could be defined, and a centrosymmetric structure would result. For emerald-green and red-brown single crystals, the six pyrophosphate groups are oriented non-symmorphically with respect to the dimer (25). The structure described by Linde in P_{ca2_1} possesses an orientation for the six pyrophosphate groups of up-up-down-down-up-down (or the converse). No model of the structure of vanadyl pyrophosphate possessing this symmetry can be constructed with less than four independent phosphorus atoms contained in the asymmetric unit of the cell. This condition forces the use of the non-centrosymmetric space group, and as will be shown below, presents an intriguing structure at the termination of the crystal parallel to the (1,0,0) surface.

Accounting for the disorder of the metal atoms in the crystallographic refinement improves the results earlier reported by Linde, but the site disorder exhibited is not simple nor statistical. The dimeric vanadium polyhedra within the crystal form a chain-like structure parallel to the a-axis, with the two independent chains lying at approximately $y = 0$ and $y = 1/2$, as illustrated in Figure 3. Interestingly, only two of the four independent vanadium sites disorder for emerald-green crystals, while all four sites disorder for their red-brown counterparts (26). In emerald-green crystals, those vanadium atom sites which lie in a chain along the c-axis at y=1/2, disorder with approximate 3:1 site occupation for the two possible positions above or below the basal plane. More massive disorder of all four vanadium sites is found for the red-brown crystals. Preliminary counter-weighted isotropic least-squares refinement of the disordered model leads to convergence at R_1=0.0344 and R_w=0.0355 for a typical green crystal, and R_1=0.0540 and R_w=0.0560 for a typical red-brown crystal. The aberrant bonding interactions reported by Linde are not present in the fully refined disordered models. For the two typical refinements noted above, the four independent vanadyl bonds average 1.604(20)Å and 1.621(13)Å in emerald-green and red-brown crystals, respectively. At this time we do not have an exact explanation of the cause of this pattern of disorder. However, considering the results in the case of the emerald-green crystal, a possible explanation of the disorder would involve the co-crystallization of two polytypes of vanadyl pyrophosphate whose structures differ in the relative orientation of adjacent dimer chains lying along y=0 and y=1/2 as illustrated in Figure 5.

There is strong evidence apparent in the single crystal step scans which indicate that the patterns of disorder of the metal atom sites in green and brown crystals follow the differences in peak intensities and

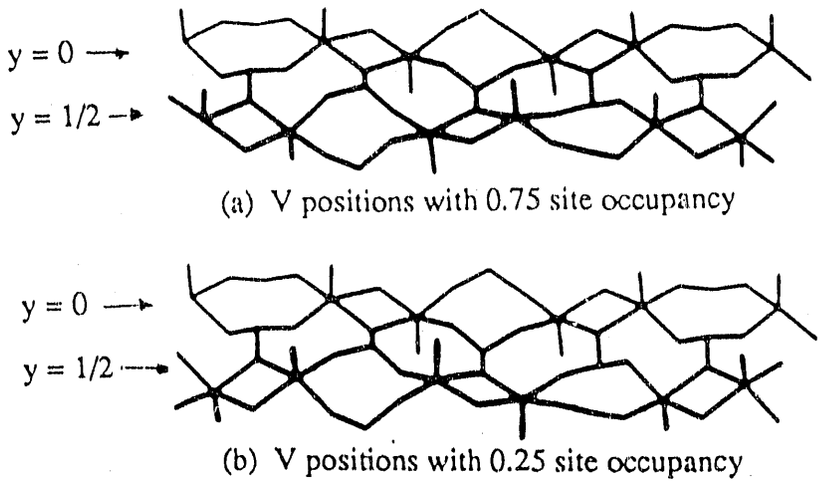

Figure 5. Models of vanadyl pyrophosphate illustrating the disordered chain structure along the crystallographic c-axis.

peak widths in X-ray powder patterns for samples prepared via differing synthetic routes. In order to determine the correlation between the single crystals and the catalyst powder patterns we have generated simulated XRD's (Figure 6), based on the convolution of individually measured intensities from the single

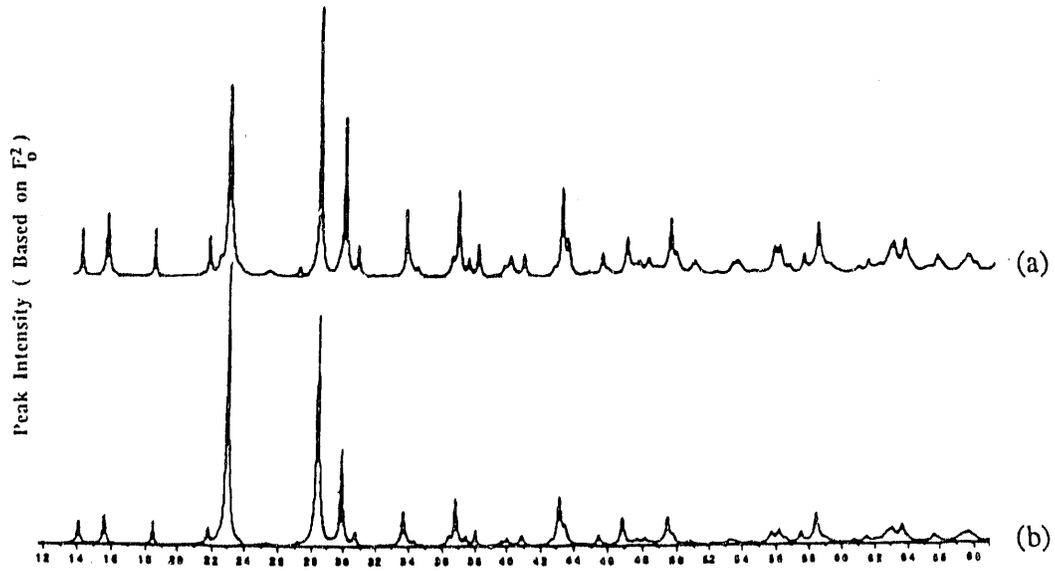

Figure 6. Calculated powder patterns based on the convolution of peak intensity and observed peak widths taken from single crystal step scans for (a) emerald green and (b) red-brown crystals.

crystal studies (27). These patterns indicate excellent correspondence with experimental patterns of catalyst samples. Convolutions generated from data derived from emerald-green crystals are representative of experimental patterns of vanadyl pyrophosphate synthesized from organic alcohol intercalated precursors, while those generated from step scans taken from red-brown crystals resemble the patterns observed from materials generated from aqueous preparation. In summary, these results provide support for the idea that

the differences in the XRD patterns between aqueous and organic derived catalysts arises from structural disordering, and this disordering is associated with the orientation of the vanadyl columns in the structure.

Models of Surface Topology Parallel to (1,0,0) and Site Isolation.

Obvious questions relate to what significance, if any, these structural attributes might have on the catalytic behavior of vanadyl pyrophosphate. We believe that both effects, namely, the asymmetric orientation of the pyrophosphate groups around the vanadium dimer, and the columnar disordering of the vanadyl moieties can have a profound structural effect on the surface topology parallel to the (1,0,0) surface.

In order to premise our models of surface topology, it is instructive to consider the simple topotactic reaction which transforms the orthophosphate precursors into the pyrophosphate phase, and the consequences of the topotaxy at the (1,0,0) surface of an isolated single crystal (28). It is important to recognize that for each intact layer of either the orthophosphate or pyrophosphate phase, the atomic P/V ratio is 1.0. In the case of the orthophosphate hemihydrate precursor, two equivalents of water are released as a result of topotaxy in the generation of the pyrophosphate phase: loss of the water of solvation and one equivalent from the dehydration of two adjacent interlayer orthophosphate groups in the formation of the pyrophosphate (P-O-P) bond. In the ordered structure of the orthophosphate precursor, half of the hydroxyl protons of the $HOPO_3^{2-}$ moieties are oriented above or below the close-packed plane. Dehydration results in half of the pyrophosphate bonds being formed in bridging positions to a layer above the plane, and half to a layer below (29). However, at the surface of this hypothetical isolated crystal, the dehydration to form the pyrophosphate bond can proceed with the formation of only one half of an equivalent: only those which will bridge between the surface and the first sub-surface layer. The surface atomic P/V ratio of this material will be identical with that of the bulk (P:V=1.0), and the surface layer will be chemically representative of a mixed orthophosphate/pyrophosphate. If the topotaxy is accomplished in excess phosphorus, as is generally the case for the material found to have the highest selectivity, the remaining surface orthophosphate can be transformed into pyrophosphate. This material would possess a surface atomic P/V ratio of 1.5, in agreement with experimental observation. We believe that these arguments are rational and chemically intuitive, and should be valid regardless of the exact nature of the topology of the (1,0,0) surface (i.e., flat or stair-step) since they are premised on the stoichometry of the compound and the topotaxy which relates the structure of the precursor to the product. Surface relaxation effects and surface reconstruction would be expected to be minor considerations due to the fact that the protonated phosphate moieties at the surface can retain full valance around each oxygen and phosphorus atom (30). The five coordinate vanadium atoms which terminate in vanadyl columns oriented into the crystal can easily solvate or chemisorb a labile sixth ligand.

When considering static models of termination of the crystal structure parallel to (1,0,0), in which all surface terminating phosphorus groups are represented as pyrophosphate moieties, the most intriguing feature relates to the manner in which the pyrophosphate groups orient about the vanadium dimer. In

particular, the direction of two pairs of two adjacent groups orient together, ie. up-up-down-down-up-down, traversing the perimeter of the dimer. Figure 7 illustrates a model of the structure parallel to (1,0,0)

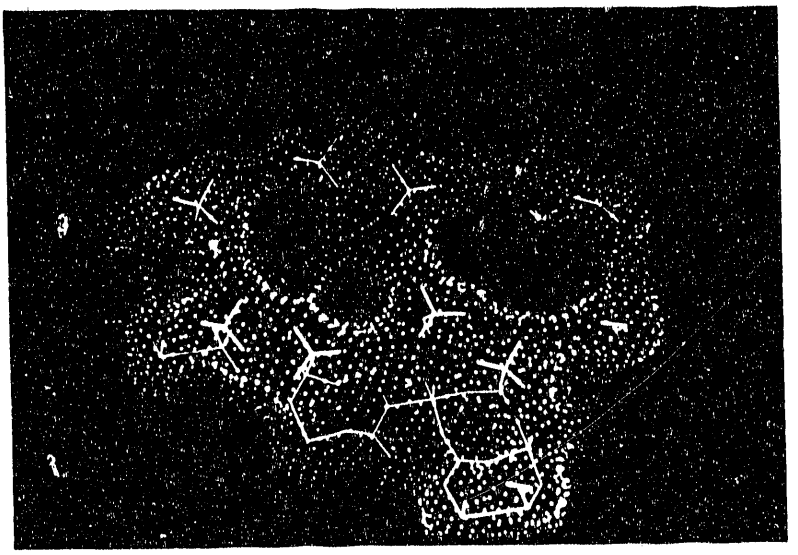

Figure 7. A model of surface termination parallel to (1,0,0) for vanadyl pyrophosphate. The dot surface is used to illustrates the accessible van der Wall surface (Connolly surface) using a probe sphere radium of 1.5Å.

and its accessible van der Waal surface (31). This model possesses a surface layer exhibiting an atomic P/V ratio of 1.5 and clearly indicates a surface cavity created by the "vacancy" of two adjacent pyrophosphate groups. This cavity is roughly elliptical in shape and the internal parimeter of the ellipse is bordered by several sets of surface terminating vanadyl groups. The vanadyl groups (or conversely, open sixth coordination sites) that are positioned at the ends of the elliptical cavity are severely hindered by two adjacent overshadowing pyrophosphate groups while others vanadyl moieties more central to the cavity are more accessible.

The importance of the directional character of the vanadyl columns, and the symmetry of the structure can be appreciated when considering models such as that shown in Figure 7. If there exist stable polytypes of vanadyl pyrophosphate (or alternatively, statistically disordered structures) which relate differing chain symmetry within the crystal, then the number, accessibility, and symmetry of unhindered vanadium coordination sites and vanadyl groups will be different for the different polytypes. We are currently exploring the structural consequences of differing eutaxy in models of vanadyl pyrophosphate in order to gain some understanding of the magnitude of the total energy differences. These calculations are being performed using an ab-initio self-consistent-field Hartree Fock formalism which fully treats crystallographic translation and symmetry (CRYSTAL, Pisani et al.) (32). These calculations may help us determine if it is rational to propose polytypes for vanadyl pyrophosphate, or whether it is more appropriate to discuss these structures in the context of statistical disorder.

Conclusions

Our structural study indicates that the vanadyl pyrophosphate compound can crystallize with varying degrees of disorder of the vanadium positions. The best description of the disordering is variability in the directional orientation of the vanadyl columns running perpendicular to the surface parallel to (1,0,0). This columnar disorder becomes very important when considering the non-stoichometric P/V surfaces parallel to (1,0,0). Terminating the surface in pyrophosphate groups places the reactive vanadium centers in cavities with varying degrees of steric hindrance by surface pyrophosphate moieties. The degree of vanadium center hindrance in the cavity is influenced significantly by the orientation and symmetry of the vanadyl columns within the structure. The analysis of the surface topology reveals an isolation of vanadium centers as surface clusters of up to four accessible vanadium centers per cavity. This model provides a means for active site isolation, an important general property for selective oxidation catalysts. First described by Grasselli (33), the site isolation principle requires that active oxygen be distributed in an arrangement that provides for limitation of numbers of active oxygen in various isolated locations so as to restrict overoxidation. Our proposed surface model encompasses both of these key features. Furthermore, it is clear from our surface model that loss of phosphorus through rupture of surface pyrophosphate groups will enlarge the surface cavities and thus expose larger expanses of accessible active oxygen leading to selectivity loss. As to the differences between organic and aqueous based catalyst preparations, this work leads to the new concept that the two catalyst systems may have surfaces parallel to (1,0,0) that differ subtly in surface topology. The distribution of accessible reactive sites associated with the surface cavities different in the two systems because of the columnar disorder differences. We suggest this difference can have a significant effect on the number of surface sites well suited for oxidation of butane to maleic anhydride.

REFERENCES

1. Operated by the Battelle Memorial Institute for the United States Department of Energy under contract DE-AC06-76RLO-1830.

2. J.R. Ebner, V. Franchetti, G. Centi and F. Trifiro, Chem. Rev., 88 (1988), 55.

3. J.R. Ebner and J.T. Gleves, in: A.E. Martell and D.T. Sawyer (Ed.), Oxygen Complexes and Oxygen Activation by Transition Metals, Plenum Press, New York , 1988, p. 273.

4. G. Centi, F. Trifiro, G. Busca, J.R. Ebner, and J.T. Gleves, in: M.J. Philips and M. Ternan (Ed.), Proc. 9th Int. Congr. Catal., The Chemical Institute of Canada, Ottawa, 1988, p. 1538.

5. M.A. Pepera, J.L. Callahan, M.J. Desmond, E.C. Millberger, P.R. Blum and M.J. Bremer,

   J. Am. Chem. Soc., 107 (1985), 4883.

6. G. Centi, F. Trifiro, G. Busca, J.R. Ebner, J.T. Gleaves, Faraday Discuss. Chem. Soc., 87 (1989), 215.

7. J. Ziolkowski, E. Bordes, P. Coutine, J. Catalysis, 122 (1990), 126.

8. G. Busca, F. Cavana, G. Centi, and F. Trifiro, J. Catal., 90 (1986), 400.

9. E. Bordes, in: Petroleum Division Preprints of the Symposium: Hydrocarbon Oxidation, 194th American Chemical Society Meeting, New Orleans, 1987, p. 792.

10. H.S. Horowitz, C.M. Blackstone, A.W. Sleight and G. Tenfer, Appl. Catal., 38 (1988), 193.

11. R.A. Schneider, U.S. Patent 4043943 (1977).

12. F. Cavana, G. Centi and F. Trifiro, J. Chem. Soc., Chem. Commun., (1985), 492.

13. J.W. Johnson, D.C. Johnston, A.J. Jacobson and J.F. Brody, J. Am. Chem. Soc., 106 (1984), 8123.

14. D.C. Johnston and J.W. Johnson, J. Chem. Soc., Chem. Commun., (1985), 1720.

15. (a) Linde, S.A.; Gorbunova, E., Dolk. Akad. Nauk, SSSR (English Trans), 245 (1979), 584; (b) Middlemiss, N.E., doctoral dissertation, Department of Chemistry, McMaster University, Hamilton, Ontario, Canada, (1978).

16. Z. Zazhigalor, V. Belousov, G. Komashko, A. Pyatnitskaya, Y. Komashko, Y. Merkureva, A. Poznyakevich, J. Stoch and J. Haber, in: M.J. Philips and M. Ternan (Ed.), Proc. 9th Int. Congr. Catal., The Chemical Institute of Canada, Ottawa, 1988, p. 1538.

17. J. Haas, C. Plog, W. Maunz, K. Mittag, K. Gollmer, B. Klopries, ibid, p. 1652.

18. (a) The space group P_{bc2_1} is a non-standard setting of P_{ca2_1}-C_{2v} (No.29), in: Theo Hahn, (Ed.), International Tables for Crystallography, Volume A, Reidel, Dordrecht, Holland (1983), p 216, (b) non-standard setting of P_{bcm}-D_{2h} (No.57), ibid, p. 277, (c) pseudo a-glide perpendicular to c is particularly strong for the red-brown materials: Pcaa is a non-standard setting of P_{cca}-D_{2h} (No. 54), ibid, p. 270.

19. Johnson, J.W.; Johnston, D.C.; Jacobson; A.J. Broady, J.F., J. Amer. Chem. Soc., 106 (1984), 8123.

20. Note the use of the standard space group setting of P_{ca2_1}-C_{2v} (No.29).

21. J.J. Freeman, Internal Monsanto Company Report.

22. The pseudo-symmetry is reflective of the site symmetry associated with the positions of the octahedral and tetrahedral intersticies of this particular type of oxide close packing.

23. E. Bordes, P. Courtine, J. Catal., 57 (1979), 236.

24. Vanadyl bond lengths have values of approximately 1.60Å, while those trans to the vanadyl oxygen are approximately 2.25-2.35Å.

25. The term "non-symmorphic" is used in this context to indicate that there is no symmetry element which can commute the six pyrophosphate moieties.

26. All heavy atom sites have been refined in cycles of full-matrix least-squares using counter-weighted data and recent versions of SHELX86 (G.M. Sheldrick in: G.M. Sheldrick, C. Kruger and R. Goddard (Eds.), Crystallographic Computing 3, Oxford University Press (1985), pp. 175-189). All disordered pairs have been constrained to have a total occupancy of 1.0 and identical isotropic thermal factors. No disorder is noted for the phosphorus atoms within the fully refined structure.

27. Steps scans from the single crystal studies were used to compute widths-at-half-height for each reflection. Peak intensity was computed from the observed structure factors whose 2θ values were placed on a wavelength scale for Cu radiation, and back-corrected for absorption (in order to simulate the powder patterns observed using Cu radiation). Convolutions of the set of peaks having $10.0^{o} \leq 2\theta Cu_{K} \leq 80.0^{o}$ utilized Lorentzian lineshapes. Experimental powder patterns have not yet been performed due to the exceedingly small amount of single crystal material obtained.

28. E. Bordes, P. Courtine, J.W. Johnson, J. Solid State Chem., 55 (1984), 270.

29. Careful consideration of the crystal structures of the orthophosphate hemihydrate indicate that some reorganization of the phosphate moieties must occur in the process of topotaxy. Powder patterns of all microcrystalline samples of the catalyst materials indicate an order of magnitude broadening of odd-odd-odd reflections. This parity group can be shown to be very sensitive to positional disordering of the phosphorus atoms within this structure. No such broadening of this parity group is seen for the single crystals.

30. Major reconstructive processes of surfaces are generally thought to be driven by surface bond rehybridization which accommodates dangling bond states caused by loss of full valance.

31. M.L. Connolly, J. Mol. Graphics, 4 (1986), 3.

32. R. Dovasi, C. Pisani, C. Roetti, M. Causa, and V.R. Saunders, Quantum Chemistry Program Exchange, Publication 577, University of Indiana.

33. R. Grasselli, in: J. Nonnelle, B. Delmon, E. Derouane (Eds.), Surface Properties and Catalysis by Non-Metals, Elsevier, Amsterdam (1983), p. 273.

END

DATE FILMED

02 / 12 / 91